Liquid Crystals
Publication details, including instructions for authors and subscription information:
http://www.informaworld.com/smpp/title~content=t713926090

Sub-millisecond transient vertical chevron formation during the electroclinic effect in the smectic A* phase

L. A. Parry-Jones[a]; S. M. Beldon[a]; P. D. Brimicombe[a]; R. M. Richardson[b]; D. Rodriguez-Martin[b]; S. J. Elston[a]; J. G. Grossmann[c]; G. R. Mant[c]
[a] Department of Engineering Science, University of Oxford, Oxford OX1 3PJ, UK [b] H H Wills Physics Laboratory, University of Bristol, Bristol BS8 1TL, UK [c] Synchrotron Radiation Department, CCLRC Daresbury Laboratory, Cheshire WA4 4AD, UK

To cite this Article Parry-Jones, L. A. , Beldon, S. M. , Brimicombe, P. D. , Richardson, R. M. , Rodriguez-Martin, D. , Elston, S. J. , Grossmann, J. G. and Mant, G. R.(2006) 'Sub-millisecond transient vertical chevron formation during the electroclinic effect in the smectic A* phase', Liquid Crystals, 33: 7, 767 — 773
To link to this Article: DOI: 10.1080/02678290600761781
URL: http://dx.doi.org/10.1080/02678290600761781

Liquid Crystals, Vol. 33, No. 7, July 2006, 767–773

Taylor & Francis
Taylor & Francis Group

Sub-millisecond transient vertical chevron formation during the electroclinic effect in the smectic A* phase

L.A. PARRY-JONES†, S.M. BELDON†, P.D. BRIMICOMBE†, R.M. RICHARDSON*‡, D. RODRIGUEZ-MARTIN‡, S.J. ELSTON†, J.G. GROSSMANN§ and G.R. MANT§

†Department of Engineering Science, University of Oxford, Parks Road, Oxford OX1 3PJ, UK
‡H H Wills Physics Laboratory, University of Bristol, Tyndall Avenue, Bristol BS8 1TL, UK
§Synchrotron Radiation Department, CCLRC Daresbury Laboratory, Warrington, Cheshire WA4 4AD, UK

(*Received 10 October 2005; in final form 14 March 2006; accepted 21 March 2006*)

X-ray diffraction studies are carried out in order to probe the smectic layer structure in liquid crystal devices filled with FLC mixture SCE8 and AFLC mixture CS4001, at a temperature just above the SmA*–SmC* phase transtion. The data gathered are time-resolved in synchronization with a bipolar voltage pulse applied across the device. The layers are observed to move dynamically and reversibly with voltage application and removal, giving evidence for temporary vertical chevron formation due to the electroclinic effect on a timescale consistent with this phenomenon.

1. Introduction

The electroclinic effect was first reported as a pre-transitional phenomenon at temperatures above the smectic A* to smectic C* phase transition in 1977 by Garoff and Meyer [1]. When an electric field is applied parallel to the layers of a smectic A* (SmA*) liquid crystal a tilt (perpendicular to the applied field) is induced in the molecular axis, its magnitude being proportional to the applied field. With a sub-millisecond response time and grey scale capabilities, the electroclinic effect has great potential as a high speed electro-optic modulator [2, 3].

In addition to a field-induced tilt in the molecular axis, a tilt can also occur as the material is cooled into the underlying smectic C* (SmC*) phase. In a planar aligned device, where the SmA* layers are originally perpendicular to the surfaces (the 'bookshelf' geometry), the phase transition is accompanied by the formation of a 'vertical chevron' structure [4], as shown in figure 1 (*a*). The vertical chevron forms because it allows the layers to become thinner as the molecules tilt relative to the layer normal, whilst retaining the layer periodicity defined by the bookshelf structure. There is also no need for any layer movement at the surface, and hence it is a relatively rapid process. In the field-induced electroclinic effect, layer shrinkage also occurs, and so in a device geometry it too might be expected to be accompanied by some kind of layer reorientation.

Let us suppose that when an electric field is applied to a SmA* bookshelf structure, the layer packing density is conserved in the same way as when the material is cooled from SmA* to SmC*, i.e. a vertical chevron is formed. However, as shown in figure 1 (*b*), the spontaneous polarization in a vertical chevron is not parallel to the applied field. Therefore there is a torque which has a tendency to cause the layers to rotate in a vertical plane. This is the same driving mechanism that causes the well known chevron to quasi-bookshelf transition at high fields in SmC* materials at any temperature. The term 'quasi-bookshelf' is used because there must be some layer-breaking as the layer packing density is destroyed, and hence a somewhat disorganized structure is formed. An alternative to the quasi-bookshelf structure is the 'horizontal chevron', in which the layers tilt within the plane of the surfaces [5, 6]. This preserves the layer packing density at the same time as aligning the spontaneous polarization with the applied field. However, unlike the vertical chevron case, the surface layers must move in order to create a horizontal chevron, so the process is relatively slow. The transition from vertical to horizontal chevron structures causes the familiar needle defects often observed in SmC* devices that have had some field treatment.

It seems logical, therefore, to expect the same kind of horizontal chevron formation as a result of the electroclinic effect in the SmA* phase, and indeed, it has been reported many times [7, 8], although it is often unclear as to whether the original bookshelf structure is

*Corresponding author. Email: robert.richardson@bristol.ac.uk

Liquid Crystals
ISSN 0267-8292 print/ISSN 1366-5855 online © 2006 Taylor & Francis
http://www.tandf.co.uk/journals
DOI: 10.1080/02678290600761781

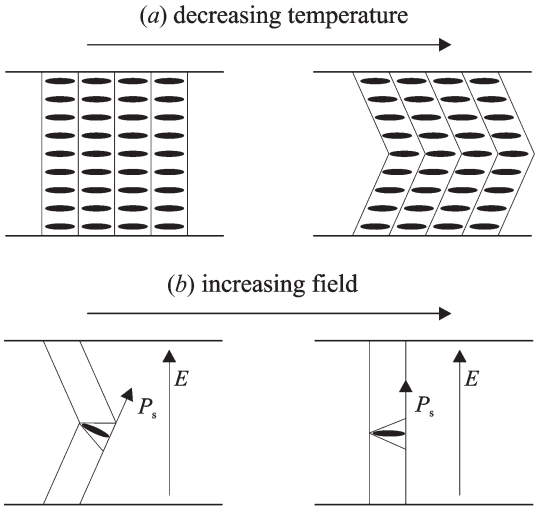

Figure 1. (*a*) Formation of a vertical chevron structure from the bookshelf structure on cooling from SmA* to SmC*. (*b*) When an electric field is applied to a vertical chevron, the spontaneous polarization is not parallel to the applied field, and hence there is a torque which might cause the layers to 'stand-up'.

regained on field removal. In one study [9], performed using microbeam time-resolved X-ray diffraction (XRD), the horizontal chevron formation occurs temporarily as the field is applied, and the original bookshelf structure is regained after field removal, on a timescale of around 50 ms.

The formation of the horizontal chevron structure requires movement of the surface layers, which can only occur on a timescale much longer than that of electroclinic switching. On the other hand, formation of the vertical chevron does not require movementof the surface layers, and is therefore a much faster process. It is therefore reasonable to suggest that a vertical chevron may form transiently during application of an electric field on a sub-millisecond timescale. Results obtained previously using XRD suggest that a vertical chevron structure may be induced by the electroclinic effect [10, 11], however this was on a much longer timescale than we are proposing. More recently, the same group have published results using time-resolved micro-beam XRD on electroclinic materials and reported both horizontal, vertical and 'compound' chevron structures, depending on the timescale and amplitude of the applied voltage waveform [12]. We have therefore carried out our own investigation into the structure present during sub-millisecond electroclinic switching in the SmA* phase on two different chiral smectic liquid crystals, one ferroelectric and one antiferroelectric at room temperature.

2. Experimental

Time-resolved X-ray diffraction experiments were carried out at Station 2.1 of the Synchrotron Radiation Source (SRS) at Daresbury Laboratories, UK [13]. This station has been used in the past to measure transient layer motion in smectic liquid crystal devices [14, 15], but far away from the phase transitions, i.e the studies were not of the electroclinic effect. Our devices suitable for X-ray scattering studies were fabricated using glass coverslips of thickness 0.1 mm (to minimize attenuation of the X-ray beam), with parallel rubbed polymer surfaces. The devices, filled with either ferroelectric liquid crystal (FLC) mixture SCE8 or anti-ferroelectric liquid crystal (AFLC) mixture CS4001, were typically 1 or 2 microns thick to ensurea strong surface influence on the bulk of the samples. The phase sequences of the two materials are as follows:

$$\text{SCE8}: \quad \mathrm{Cr}(-15)\mathrm{SmC}^*(59)\mathrm{SmA}^*(79)\mathrm{N}^*(100)$$

$$\text{CS4001}:$$

$$\mathrm{Cr}(-70)\mathrm{SmC}^*_{\mathrm{A}}(67)\mathrm{SmC}^*_{\gamma}(68)\mathrm{SmC}^*(70)\mathrm{SmA}^*(86)\mathrm{I}(^\circ\mathrm{C})$$

from which it can be seen that although CS4001 has underlying antiferroelectric and ferrielectric phases, the phase immediately below the SmA* phase is SmC*. Therefore in both cases, the study of the electroclinic effect is carried out around the SmA*–SmC* phase transition.

The X-ray beam was of wavelength 0.154 nm, and the experiment was carried out in the Bragg geometry (see figure 2). The waveform applied to the sample was generated by a Wavetek 395 arbitary waveform generator. This was triggered by the time frame generator in the data aquisition system of the beam-line station. The rotation of the sample stage, the sample temperature (controlled by a heating stage) and the data aquisition were all controlled via JPython script files. In order to be sure that the cell was at the correct temperature to exhibit the electroclinic effect (i.e. just above the SmA*–SmC* phase transition), it was useful to observe both the sample texture and electro-optic response between crossed polarizers without removing the cell from its heating stage. In order to do this, the experimental arrangement shown in figure 2 (*a*) was used. By rocking the cell into one of two specific positions, it was possible to observe either the texture or the electro-optic response before performing the X-ray measurements themselves (which would in general be at a set of different rocking angles). The texture of the sample was monitored using a polarizing zoom microscope (Leica) with a TV camera and a data capture card, whereas the electro-optic response was measured using a laser, polarizers and photodetector.

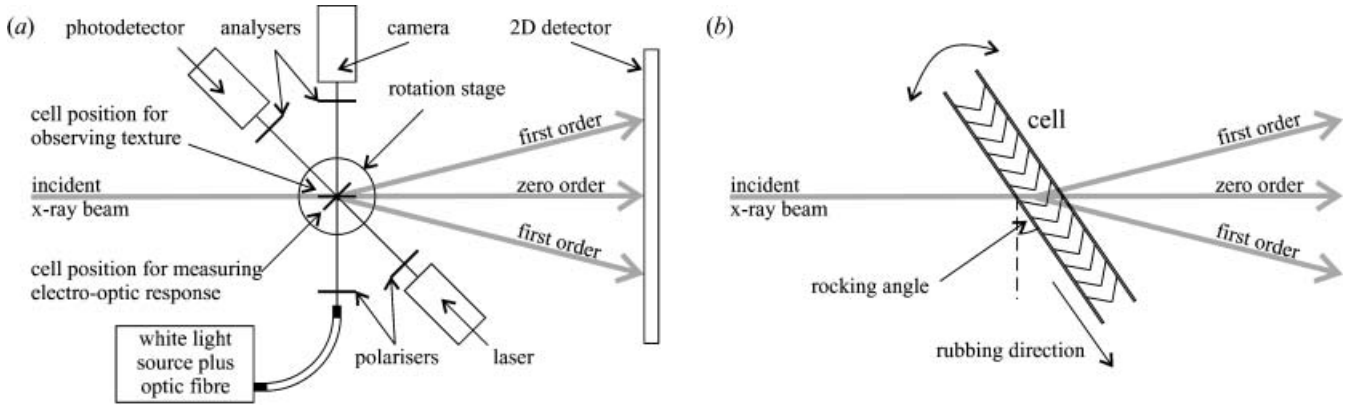

Figure 2. Illustration of the experimental arrangement used for the X-ray diffraction studies. (*a*) Shows the positions of the laser and photodetector used to measure the electro-optic response of the cell, and the white light source and camera used to monitor the texture of the cell *in situ*. This arrangement is very useful as it is necessary for the cell to be just above the SmA*–SmC* phase transition in order for the electroclinic effect to be observed. (*b*) Shows in detail the Bragg geometry used: the cell is rocked about an axis that is normal to both the incident X-ray beam and the rubbing direction (i.e. into the page). For each angle, the X-ray scattering pattern is recorded by a 2D detector.

Both liquid crystal materials SCE8 and CS4001 exhibit an electroclinic effect close to the SmC* to SmA* phase transition, and form a vertical chevron structure on cooling into the SmC* phase. Figure 3 shows the electro-optic characteristics of both materials at a temperature just above the SmA*–SmC* phase transition. It is clear that, for the same applied voltage, the AFLC CS4001 shows a much greater modulation of the transmitted intensity than the FLC SCE8, implying a stronger electroclinic effect. This was verified by rotating the cell to extinction between crossed polarizers at the two voltage extrema $\pm 10\,\mathrm{V}$ and noting the azimuthal angle difference. In SCE8 the optical tilt angle for $\pm 10\,\mathrm{V}$ was found to be $\pm 1^{\circ}$, whereas in CS4001 it was $\pm 5^{\circ}$, both at the same temperatures used to gather the data shown in figure 3. This therefore confirms that the increased electro-optic modulation shown by CS4001 is indeed due to a larger change in the optic axis, i.e. a stronger electroclinic effect. It is likely that this is because the spontaneous polarization (P_s) for the two materials is very different: they are measured to be $80\,\mathrm{nC\,cm^{-2}}$ for CS4001 and $8\,\mathrm{nC\,cm^{-2}}$ for SCE8, both at room temperature. Although the spontaneous polarization is zero in the smectic A phase, the larger room temperature value for CS4001 suggests that it will have a greater susceptibility to field induced structural changes.

Figure 4 shows the waveform applied to the cells during the X-ray experiment. A bipolar pulse of 20 V amplitude and 500 µs duration (for each sign) was applied every 10 ms, i.e. there was 9 ms rest between pulses. The X-ray data acquisition was separated into time bins of varying length, and synchronized with the applied waveform. Bin 1 was for the 500 µs period immediately before the bipolar pulse, bin 2 for the 500 µs where +20 V is applied, and bin 3 for −20 V applied. For the SCE8 cell, figure 4 (*a*), the remaining 8.5 ms was placed into bin 4, whereas for the CS4001 cell, Figure 4 (*b*), where the experiment was performed at a later date, the 500 µs immediately after the bipolar pulse was placed into bin 4, and then the remaining 8.0 ms into bin 5, so that the timescale of the layer relaxation could be assessed. The pulse length of 500 µs for each half of the bipolar pulse was chosen to be long

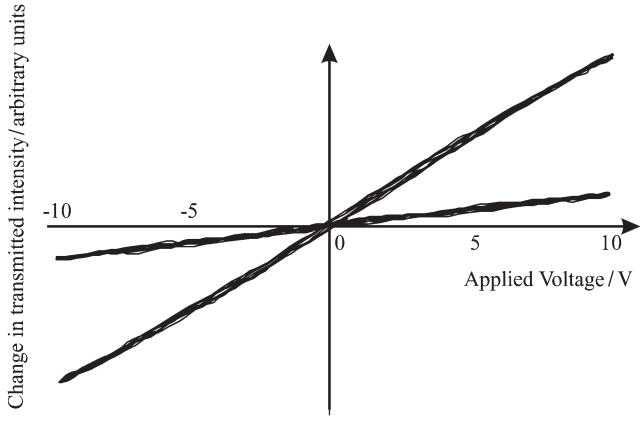

Figure 3. Comparison of the electro-optic characteristics of the electroclinic effect in SCE8 and CS4001. In both cases, the temperature of the cells is just above the SmA*–SmC* phase transition, and the rubbing direction is aligned at an angleof 22.5° to one of a pair of crossed polarizers. The change in the transmission of the cells (as compared with that at zero volts) through crossed polarizers is plotted as a function of voltage, where the applied waveform is a triangular wave offrequency 250 Hz and 10 V amplitude.

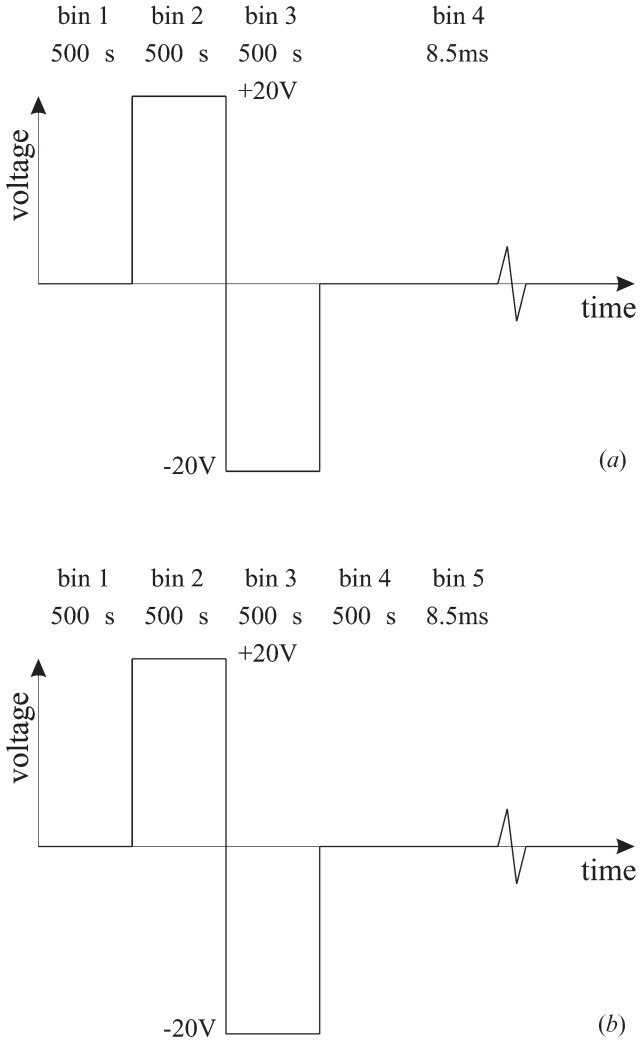

Figure 4. Illustration of the waveform applied to the liquid crystal devices: a bipolar pulse of 20 V amplitude and 500 µs duration (for each sign) is applied every 10 ms. The X-ray data aquisition at the 2D detector is synchronized with the waveform, and is divided into bins, so that the layer structure with the voltage on can be compared with the layer structure with the voltage off. (*a*), (*b*) Show the slightly different binning used for the SCE8 and CS4001 devices, respectively.

enough in order to saturate the electroclinic tilt angle and allow for any vertical layer deformation, yet short enough so that plastic irreversible processes (such as the permanent formation of horizontal chevrons) should not occur. Indeed, on application of such a waveform in the laboratory no needle defects were observed, confirming that no permanent horizontal chevron structure has formed. The long rest between pulses was allowed in case the relaxation of the director and layers back to the unperturbed bookshelf SmA* phase took longer than the 'switch-on' process: this was later found not to be the case. Data were collected over a range of rocking angles (see figure 2), at least -15° to $+15^\circ$ in 0.5° steps. In order to build up good counting statistics from the thin cells, data were gathered over 2 000–4 000 cycles of the waveform, corresponding to 1–2 s of data for each of the 500 µs bins.

3. Results

The results of the experiment on an SCE8 just above the SmA*–SmC* phase transition are shown in figure 5: (*a*), (*b*), (*c*) and (*d*) correspond to data bins 1–4, respectively, i.e. 0 V, +20 V, −20 V and 0 V applied. The contour plots show the distribution of layer normals present in the area of the device probed by the X-ray beam. The angles γ and δ represent the twist and tilt of the layer normal, respectively, as illustrated in figure 6. The method of reducing the scattering data to layer normal distributions is reported elsewhere [16]. Figure 6 (*a*) shows that at 0 V the layer normal distribution peaks at $\delta=0$, $\gamma=90^\circ$, meaning that the layers form a bookshelf structure with the layers oriented perpendicular to the rubbing direction. The data for bin 4, the 8.5 ms rest period at 0 V, show a similar result. Figures 6 (*b*) and 6 (*c*) show that subsequent application of a 20 V bipolar pulse across the cell causes some layer movement, with a peak present at $\delta\approx+4.5^\circ$. This suggests a tilting of the layer of 4.5° from the normal to the cell surface, although if a vertical chevron structure were present then one would expect a peak of similar intensity at $\delta\approx-4.5^\circ$ which is not the case, notwithstanding a spreading of the central peak towards negative values of δ. It is important to note that, although the data are not representative of a clear vertical chevron, there is distinct layer motion, and this is in the vertical plane, i.e. there is no observed tendency towards horizontal chevron formation on this timescale, as anticipated. This vertcial layer motion, or tilt, was observed to be highly temperature dependent. The same experiment, repeated 3 degrees higher in temperature showed no observable influence from the applied field, the layer normal distribution remaining strongly peaked at $\delta=0$, $\gamma=90^\circ$, i.e. the much reduced electroclinic effect at this temperature does not cause the layers to move out of the bookshelf configuration.

Figure 7 shows an equivalent set of results for a CS4001 filled cell at a temperature just above the SmA*–SmC* phase transition. Figure 7 (*a*) shows that at 0 V, the layer structure of the AFLC cell is a 'random bookshelf' structure — that is, the layers are perpendicular to the surfaces (hence $\delta=0$) — but that they are widely distributed (up to about $\pm30^\circ$) about the rubbing direction ($\gamma=90^\circ$). However, here the dynamic formation of a vertical chevron is clearly evident in figures 7 (*b*) and 7 (*c*). In this case, it is apparent that

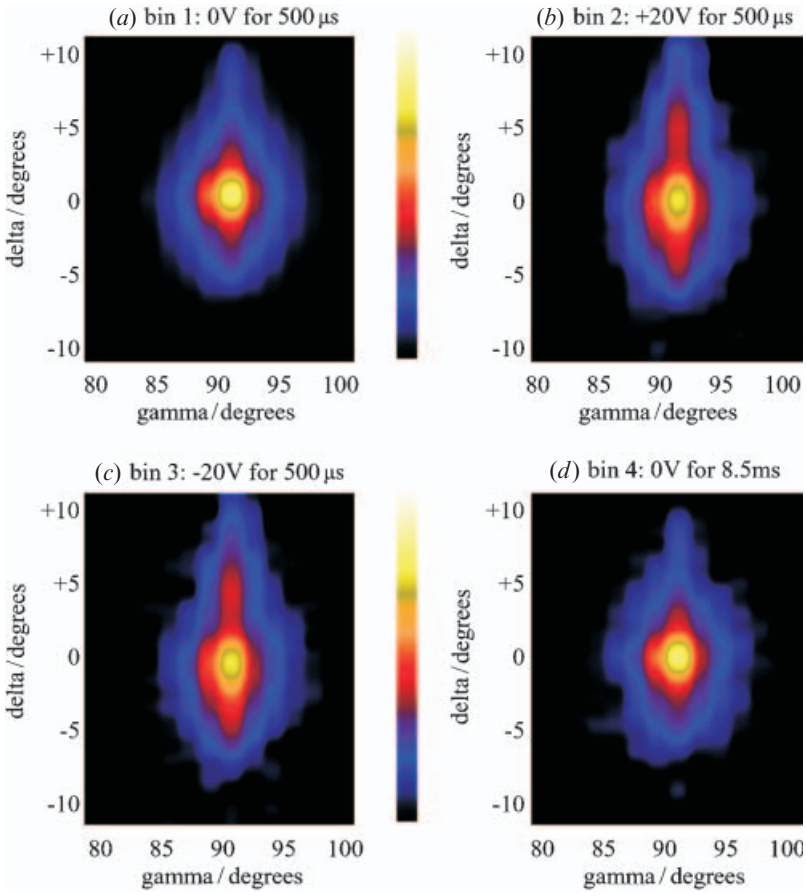

Figure 5. Comparison of the experimental results for the SCE8 cell just above the SmA*–SmC* phase transition for (*a*) bin 1: 0 V for 500 µs, (*b*) bin 2: +20 V for 500 µs, (*c*) bin 3: −20 V for 500 µs, (*d*) bin 4: 0 V for 8.5 ms. The axes of the plots are illustrated in figure 6, and the colour bars shown in the centre of the figure show the order of the false colours used on the logarithmic contour plots.

although some of the device remains in the bookshelf structure, a significant proportion forms a chevron structure, shown by the peaks at $\delta = \pm 2.5^\circ$. (We hypothesise that the regions which remain in the bookshelf configuration are the defect regions between domains of uniform later orientation, which are less free to move than those layers inside a well aligned domain). Figure 7 (*d*) shows the data gathered in the 500 µs period immediately after the bipolar pulse. It is interesting to note that the layer normal distribtion seems to be entirely bookshelf again, within an extremely short time. It appears that the layers are tilting (and 're-bookshelfing') on a timescale comparable with the electroclinic effect itself, as originally hypothesized.

For comparison of the two materials, figure 8 shows cross-sections taken through the voltage-on contour plots at $\gamma = 90^\circ$, for both materials. Whereas for SCE8 the dynamic layer redistribution is relatively subtle, the formation of a vertical chevron structure in some parts

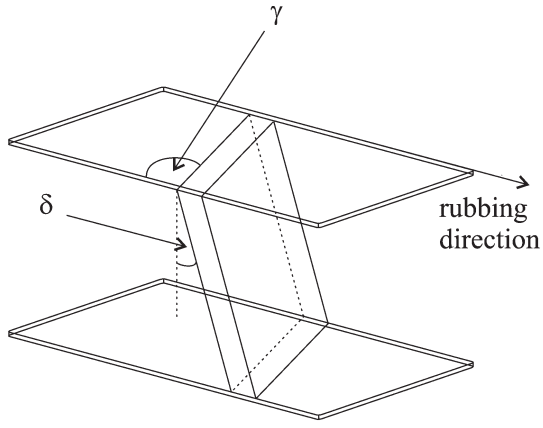

Figure 6. Illustration of the meaning of the angles δ and γ used in the description of the smectic layer normal distribution. δ is the tilt of the layers away from the bookshelf configuration, and the twist angle γ is defined to be 90° when the layer normal is aligned with the rubbing direction.

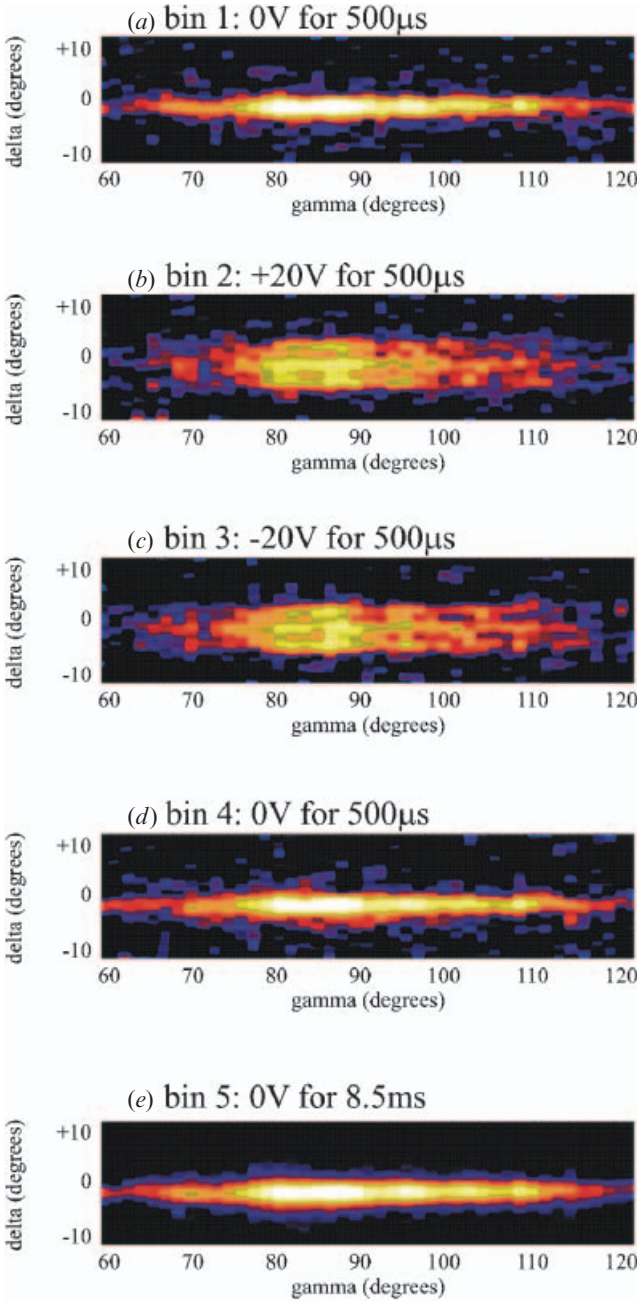

Figure 7. Comparison of the experimental results for the CS4001 cell just above the SmA*–SmC* phase transition for (*a*) bin 1: 0 V for 500 µs, (*b*) bin 2: +20 V for 500 µs, (*c*) bin 3: −20 V for 500 µs, (*d*) bin 4: 0 V for 500 µs, (*e*) bin 5: 0 V for 8 ms. The order of the colours used in the logarithmic contour plots is the same as in figure 5.

of the device is very clearly indictated by the three separate peaks in the data for CS4001. We conclude that the effect is more evident in CS4001 compared with SCE8 because the strength of the electroclinic effect is much greater in the AFLC material, probably due to the much higher spontaneous polarization.

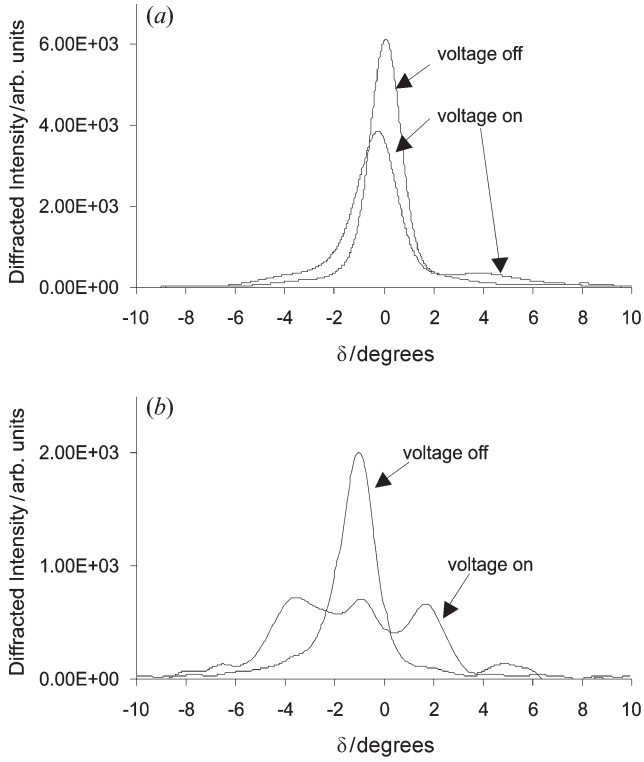

Figure 8. Cross-section taken through the voltage-on contour plots at $\gamma=90^{\circ}$ for (*a*) SCE8 and (*b*) CS4001. Note that SCE8 shows a subtle transient change to its original bookshelf structure, whereas CS4001 shows very distinctly that, whilst some areas remain in the bookshelf configuration, others form a vertical chevron structure.

4. Conclusion

The results presented here show a dynamic vertical chevron formation during electric field application in planar aligned devices filled with two different types of liquid crystal material, FLC SCE8 and AFLC CS4001. This reversible layer rotation occurs on a sub-millisecond timescale, and relaxes back to the bookshelf configuration within a few milliseconds. Further, we note that for CS4001, the re-bookshelfing occurs on a similar timescale to the chevron formation, i.e. sub-millisecond. It is therefore clear that, when the applied voltage pulses are sufficiently short, there is not insuffi time for horizontal chevron formation; the layer packing density is conserved during electroclinic switching via vertical chevron formation.

Acknowledgements

The authors would like to acknowledge the financial support of the EPSRC, Sharp Laboratories of Europe (SLE) and the Royal Society. We would also like to

thank Emma Walton of SLE, for help in device fabrication.

References

[1] S. Garoff, R.B. Meyer. *Phys. Rev. Lett.*, **38**, 848 (1977).
[2] G. Andersson, I. Dahl, L. Komitov, S.T. Lagerwall, K. Sharp, B. Stebler. *J. Appl. Phys.*, **66**, 4983 (1989).
[3] S.T. Lagerwall, G. Andersson, I. Dahl, W. Kuczynski, K. Sharp, B. Stebler. 1989: U. S. Patent No. 4 838 663.
[4] T. Reiker, N.A. Clark, G. Smith, D. Parmar, E. Sirota, C. Safinya. *Phys. Rev. Lett.*, **59**, 2658 (1987).
[5] I. Dierking, J. Giesselmann, J. Schacht, P. Zugenmaier. *Liq. Cryst.*, **19**, 179 (1995).
[6] I. Dierking, B. Gluesen, S.T. Lagerwall, C.K. Ober. *Phys. Rev. E*, **61**, 1593 (2000).
[7] A.G. Rappaport, P.A. Williams, B.N. Thomas, N.A. Clark, M.B. Ros, D.M. Walba. *Appl. Phys. Lett.*, **67**, 362 (1995).
[8] R.E. Geer, S.J. Singer, J.V. Selinger, B.R. Ratna, R. Shashidhar. *Phys. Rev. E*, **57**, 3059 (1998).
[9] Y. Takahashi, A. Iida, Y. Takanishi, M. Nakata, K. Ishikawa, H. Takezoe. *Ferroelectrics*, **311**, 41 (2004).
[10] M. Johno, A.D.L. Chandani, Y. Takanishi, Y. Ouchi, H. Takezoe, A. Fukuda. *Ferroelectrics*, **114**, 123 (1991).
[11] Y. Takahashi, A. Iida, Y. Takanishi, T. Ogasawara, K. Ishikawa, H. Takezoe. *Mol. Cryst. liq. Cryst.*, **365**, 853 (2001).
[12] A. Iida, Y. Takahashi, Y. Takanishi, M. Nakata, K. Ishikawa, H. Takezoe. *Liq. Cryst.*, **32**, 717 (2005).
[13] E. Towns-Andrews, A. Berry, J. Bordas, G.R. Mant, P.K. Murray, K. Roberts, I. Sumner, J.S. Worgan, R. Lewis. *Rev. sci. Intrum.*, **60**, 2346 (1989).
[14] H.F. Gleeson, A.S. Morse. *Liq. Cryst.*, **21**, 755 (1996).
[15] H.F. Gleeson, G.K. Bryant, A.S. Morse. *Mol. Cryst. liq. Cryst.*, **362**, 203 (2001).
[16] S. Jenkins, J. Jones, P. Dunn, S. Haslam, R. Richardson, L. Taylor. *Mol. Cryst. liq. Cryst.*, **329**, 19 (1999).